Property Self-Optimization During Wear of MoS2

DOI:
10.1021/acsami.6b13802

Document Version
Accepted author manuscript

Property Self-Optimization During Wear of MoS_2

Rui Hao,[a] Aleksander A. Tedstone,[b] David J. Lewis,[c] Chris P. Warrens,[d] Kevin R. West,[d] Philip Howard,[d] Sander Gaemers,[d] Shen J. Dillon,[a,*] and Paul O'Brien,[b,*]

[a] International Centre for Advanced Materials (ICAM; UIUC Spoke), Frederick Seitz Materials Research Laboratory, University of Illinois at Urbana−Champaign 104 South Goodwin Avenue, MC-230, Urbana, Illinois 61801, United States

[b] International Centre for Advanced Materials (ICAM; Manchester Hub), School of Chemistry, University of Manchester, Oxford Road, M13 9PL, United Kingdom.

[c] International Centre for Advanced Materials (ICAM; Manchester Hub), School of Materials, University of Manchester, Oxford Road, M13 9PL, United Kingdom.

[d]BP Technology Centre, Whitchurch Hill, Pangbourne, Berkshire, RG8 7QR, United Kingdom.

Keywords: antiwear films, tribology, in situ electron microscopy, transition metal dichalcogenides, molybdenum disulfide.

ABSTRACT: Knowledge of their bulk physical properties often guides selection of appropriate tribological coating materials. However, these properties as well as the microstructure evolve dramatically under the extreme conditions imposed during mechanical wear. The dynamic response ultimately governs the material's wear performance and thus understanding the dynamic evolution of the system is critical. This work characterizes the change in mechanical properties and microstructure as a function of wear cycles in model MoS_2 films using a combination of nano-wear testing, transmission electron microscopy, and site-specific nano-pillar compression. Notably, mechanical wear enhances the mechanical properties of the MoS_2, while simultaneously evolving a microstructure that reduces the coefficient of friction and wear rate. We hypothesize that this self-optimizing behavior underpins the exceptional lubricity and anti-wear performance of MoS_2.

Introduction

Molybdenum(IV) disulfide (MoS_2), graphite, and related layered materials provide excellent solid lubrication between surfaces (coefficient of friction < 0.1). This property derives from their structures in which weaker van der Waals bonding between 2-D layers of in-plane covalently bonded atoms enable low energy slip that reduce friction.[1-6] MoS_2 is an important solid lubricant because of its exceptional lubricity and the fact that it can easily be coated onto objects by physical vapor deposition (PVD) or chemical vapor deposition (CVD), and forms in-situ by the tribochemical reaction of molybdenum alkyldithiocarbamates,[7-8] the latter which are commonly used additives in lubricating oil formulations.[9-10] Most CVD and PVD processes allow for great flexibility in tuning the chemistry and/or structure of the solid lubricant film, and consequentially tailoring its properties. A number of studies have utilized this method to improve the understanding of the wear behavior of MoS_2, by altering the bonding between MoS_2 sheets, varying the crystal structure and microstructural length scales, or incorporating oxygen buffers.[10-11] The definition of a clear set of design criteria for optimizing lubricity in MoS_2 remains challenging since the system evolves significantly during high cycle wear. Hypervalent dopants have been used to strengthen bonding between MoS_2 layers, which contributes to enhanced hardness[12] which should enhance for antiwear behavior, although inhibition of slip in such materials might negatively impact lubricity the deformation (e.g. ductile versus brittle). Predicting the response requires an improved understanding of how the system's microstructure and properties evolve during wear. The properties of pristine and model MoS_2 systems have been investigated in great detail and the general evolution of MoS_2 solid lubricants during high cycle wear is understood qualitatively.[10, 13] However, the associated changes in the materials properties and deformation modes during wear is not known quantitatively. High strain deformation characteristic of wear processes can significantly alter microstructure, crystal structure, and local chemistry. Optimizing the structure and chemistry of the pristine material may not provide the optimal behavior in the regime of high strain. Therefore, understanding how the structure and properties of MoS_2 evolve during wear will inform improved system design.

The structure of CVD and PVD grown MoS_2 films on alloys and their evolution during strain has been summarized previously[13]; vapor-deposited MoS_2 tends to grow with a columnar–fiber zone adjacent to the substrate, on top of which grows a morpholgically equiaxed transition region, and a ridged surface region. The films often contain significant void space and wear begins with compression of these voids. During subsequent wear the (0002) planes tend to align along the shear direction that is in most cases normal to the surface. The length scale of crystallites may refine during this period and the overall wear rate tends to be low and approximately constant. Each wear cycle increases the amount of oxygen incorporated into the film. This oxygen tends to bind to the edges of MoS_2 sheets and embrittles the material. Material transfer to asperities and cleavage of sections of the film facilitate material loss. Some of this material may be incorporated into a third body layer that can extend the lifetime of the tribolayer, but is also susceptible to cleavage. Eventually, the coating fails to prevent contact to the underlying substrate and degrades rapidly. These general trends have been confirmed via advanced in-situ and ex-situ characterization.[12, 14-19] However, the mechanisms associated with most of these processes remain unclear as do their effects on the associated materials properties. More importantly, it remains to be understood what underlying characteristics of the MoS_2 system make it a robust solid lubricant under a

variety of operational conditions for materials prepared by various methods with disparate microstructures.

In this work, we seek to quantify the mechanical properties of CVD-grown MoS_2 as they evolve during idealized dry sliding wear, elucidate the mechanical failure mechanisms associated with the MoS_2 at different stages of wear, and correlate this information with microstructural evolution. The study combines the use of microscale tribological testing that simulates asperity contact and provides well controlled and reproducible wear response with in-situ observation of nanoscale mechanical deformation of site-specific pillars fabricated from the worn material. The approach allows us to quantify the properties of the material at controlled levels of wear and provides insights into how the MoS_2 films function during wear to provide exceptional lubricity.

Experimental

Sample preparation:

MoS_2 films were grown on Si substrates that contain a flat plateau region 1 µm wide and several mm in length sitting 30 µm above the surrounding region. Figure 1 depicts this geometry schematically. This plateau region is convenient for preparing nanopillars for in-situ testing that can be imaged in cross-section. The surrounding substrate region can be used for bulk tribological testing and film characterization. The substrates were oxygen-annealed at 1100 °C to form a ≈30 nm SiO_2 barrier layer. A ≈50 nm film of 1% Cr doped-Fe was deposited onto the pre-oxidized substrate using commercial E52100 alloy steel target by magnetron sputtering. MoS_2 layers of ≈2-4 µm were deposited on the prepared substrates via Aerosol Assisted Chemical Vapour Deposition (AACVD). The AACVD process used has been described in detail previously.[12, 20] Tetrakis(*N*,*N*-diethyldithiocarbamato) molybdenum(IV) (MoL_4: 0.2 g, 0.29 mmol)) was dissloved in tetrahydrofuran (THF: 25 mL) in a 2-neck round bottom flask. An aerosol of the precursor solution generated by piezoelectric nebulisation in the flask. This was carried by a stream of argon flowing at a rate of 160-180 $cm^3\ min^{-1}$ into a quartz tube furnace. MoS_2 deposition onto the prepared substrates was performed at 500 °C for 100 min.

Pre-wear

Pre-wear was accomplished by cyclic scratch tests using a 5 µm radius conospherical tip. The load and displacements were controlled by a Hysitron TI 950 TriboIndenter. Linear reciprocating wear tests were performed between 1 to 40 complete back-and-forth cycles. The trace length was fixed to 10 µm with a tip speed of 1 µm s^{-1}. Tests were preformed with loads varying between 0.1 to 3 mN. Tests were carried out on both the 1 µm wide plateau region of the substrate and the adjacent large area flat regions of the substrate. The material in the plateau region was used for subsequent in-situ nanomechanical testing.

Characterization and in-situ testing

A focused ion beam microscope (FIB, FEI Helios 600i) was used to prepare both cross-sectional TEM specimens and pillars for nanocompression testing. Site-specific pillars were prepared via annular milling in regions of pristine and pre-worn materials to be 200 - 400 nm in diameter and 1.5 – 3 µm (including 500-800 nm MoS_2 on top) in height. Both transmission electron microscopy (TEM) characterization and *in-situ* mechanical testing were carried out in a with a Jeol 2010 LaB_6. A Hysitron PI95 TEM Picoindenter outfitted with a 2 mm diameter flat diamond punch was utilized for nanomechanical testing. The pillars were compressed under displacement control and were imaged simultaneously in bright-field. The mean mechanical property values averaged from multiple tests are reported along with standard deviations that are reported as values of experimental error. Figure 1 provides schematic diagrams demonstrating the overall sample preparation and testing procedure.

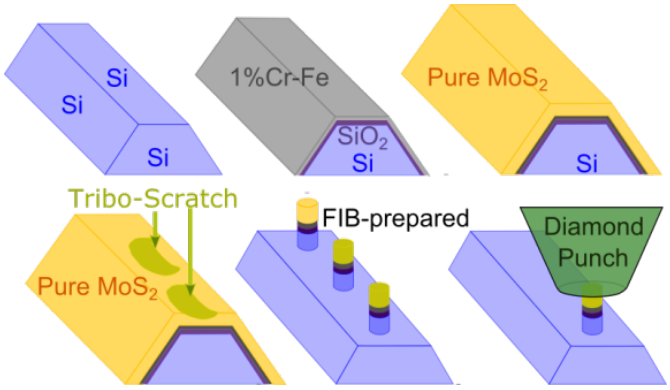

Figure 1. Sample preparation for TEM *in-situ* mechanical compression. Oxygen-annealing at 1100 °C creates a SiO_2 barrier layer, followed by magnetron sputter deposition of 1% Cr doped-Fe from an E52100 alloy steel target. MoS_2 layers of were deposited by AACVD of MoL_4, followed by tribo-scratch tests and FIB milling to create pillars of material for picoindentation.

Results

The secondary electron SEM images of MoS_2 on both the plateau region and the adjacent flat substrate in both the pristine and worn conditions after various numbers of cycles at 1 mN (Figure 2). Figure 2 also depicts cross-sections demonstrating reductions in sample thickness that are consistent with displacement measurements obtained from the Triboindentor. Most of the reduction in thickness during the first cycle results from plastic compression of the film, ie. inelastic compression of voids and alignment of lamellar crystallites.

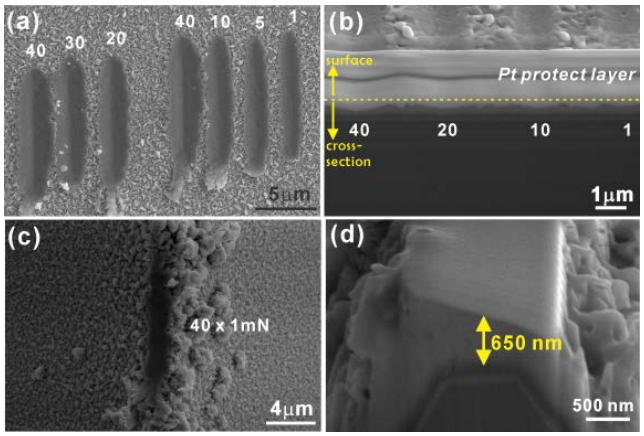

Figure 2. (a) SEM of Tribo-scratches performed at 1 mN load in the flat region of the substrate at various cycle lengths shown above each region. (b) FIB cross-section of selected tribo-scratches. (c) SEM of a 40-cycle tribo-scratch performed at 1mN load on the plateau section of the substrate. (d) FIB cross-section of tribo-scratch depicted in 2(c).

The lateral and vertical displacement of the diamond tip during wear at 1 mN are plotted in Figure 3(a) and 3(b) for both the flat and plateau regions of the substrate, respectively. Note that the images in Figure 3 are shown at different magnifications. The wear results are similar in both locations, although higher roughness is observed in the trace taken from the plateau region. The coefficient of friction (Figure 3(c)) and the wear rate per cycle

(Figure 3(d)) both decrease as the number of cycles increases. The wear rate, measured between cycles 11 to 40 and 21 to 40, decreases linearly with applied load, as anticipated, down to ca. 0.5 mN. Below this value the wear rate is negligible and much of the reduction in film thickness during the early cycles can be attributed to compression only. Cyclic wear above 5 mN causes the diamond tip to closely approach or contact the underlying substrate.

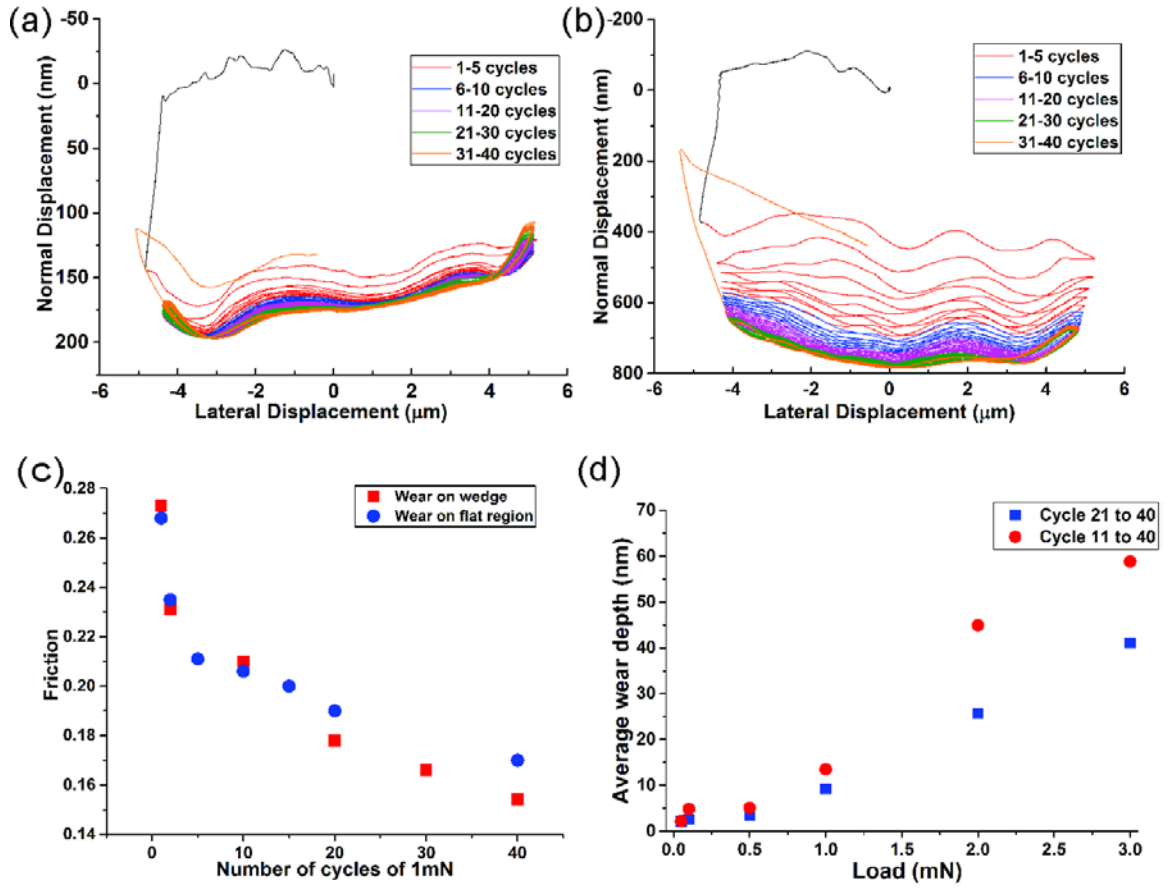

Figure 3. Lateral vs normal displacement during cyclic wear on (a) the flat section on the edge of the substrate and (b) the plateau in the center of the substrate. (c) Coefficient of friction vs. number of wear cycles for wear conducted on the flat and plateau regions of the substrate. (d) Average wear depth vs load during different parts of the wear experiment on the flat section on the edge of the substrate.

Figure 4 shows example microstructures of the as-grown MoS_2. The 150 nm area adjacent to the substrate consists of a low density packing of ca. 2-10 nm diameter 100 nm long crystallites that are disordered but with a preference toward the (0002) planes being oriented perpendicular to the substrate (Figure 4 (b)). Note that the pillars prepared for nano-compression testing consist primarily of material from this region, and typically deform and fail in this region. The 300 nm region above this is higher density and is composed of ca. 25 nm diameter columnar crystallites strongly oriented with their (0002) planes perpendicular to the substrate. The near surface region is lower density with large pores and more randomly oriented coarse crystallites. The general microstructure is similar to other vapor-deposited MoS_2 films reported in the literature.[13] After pre-wear of the samples to 40 cycles at 1 mN, MoS_2 crystallites in the near substrate region align their (0002) planes more parallel to the substrate (Figure 4 (c)). The region is compressed in the axial direction by ≈15%, indicating densification of this material. In the region above, the microstructure is similar to the pristine samples, with the only pronounced reorientation of the crystallites in the near surface region, which is now compressed with the (0002) planes reoriented parallel to the surface and shear direction. During wear at 3 mN, the crystals in the center columnar region also reorient (Figure 4 (d)) to align their (0002) toward the shear direction. This behavior is consistent with prior cross-sectional TEM observations of worn MoS_2.[17]

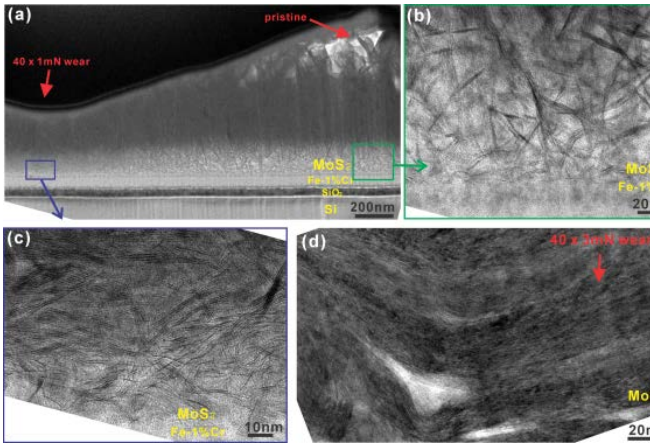

Figure 4. TEM Micrographs of MoS_2. (a) Cross-section through the wear track produced by 40 cycles of 1 mN wear of AACVD-grown MoS_2 film on Si/SiO_2/Fe-1% Cr substrate. (b) Cross section of as-grown AACVD MoS_2 showing randomly oriented crystallites (c) Cross section of AACVD-grown MoS_2 after 40 cycles of 1mN wear showing axial compression and alignment of crystallites with wear direction (d) Cross section of AACVD-grown MoS_2 after 40 cycles of 3mN wear showing further axial compression and reorientation of crystallites

Site-specific nano-pillars were prepared from the regions of material pre-worn for 0, 10, 20, and 40 cycles. Figure 5 shows example time-lapse images of *in-situ* TEM nanocompression performed on these samples. The pristine samples fracture catastrophically with a yield strength of 0.97 ± 0.02 GPa. The yield strength increases with an increasing number of pre-wear cycles up to 1.19 ± 0.03 GPa. This data is plotted in Figure 6 along with values of apparent moduli, which also increase with pre-wear cycle number. Here the modulus is taken as the slope of the stress-strain curve, which does not account for contributions of the diamond indenter and the silicon substrate. It can be noted from the time-lapse images that the deformation mode becomes increasingly ductile with pre-wear, where the strain to fracture increases with the number of wear cycles.

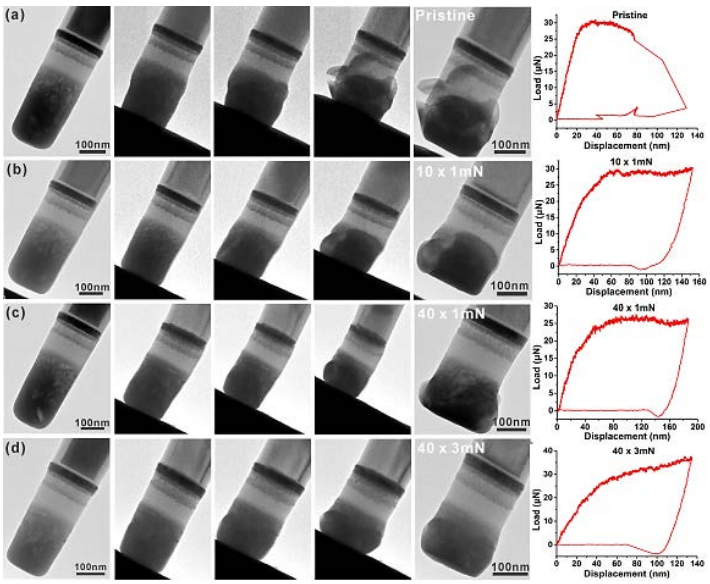

Figure 5. Time-lapse images of in-situ TEM nanocompression after different levels of pre-wear (a) Pristine MoS2 (b) Pre-worn by 10 cycles of 1 mN wear (c) Pre-worn by 40 cycles of 1 mN wear (d) Pre-worn by 40 cycles of 3 mN wear.

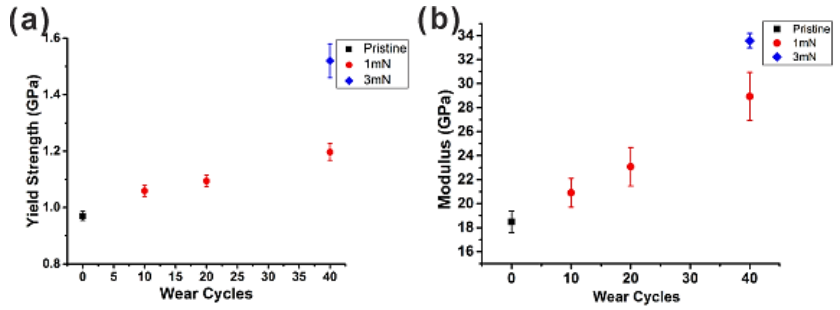

Figure 6. Evolution of (a) yield strength and (b) modulus of MoS_2 nanopillars fabricated from thin films with increasing numbers of wear cycles

To better understand how deformation affects crystallite orientation, *in-situ* electron diffraction was performed during compression. This allows us to characterize the evolution of the crystallographic texture during loading. The results indicate that the sample does not fail catastrophically until the basal planes preferentially align approximately 45° to the loading axis. This is true of both the pristine material (Figure 7) and the pre-worn material (Figure 8), where the latter is textured such that the (0002) planes are aligned with the substrate and the former has its (0002) planes textured normal to this direction. In both cases, the (0002) planes try to realign to the direction of principal shear. This correlates with the behaviour during pre-wear, where the principal shear aligns the particles with the substrate. For perfect shear, a strain of 1 would be required to reorient the crystals 45 °. However, a significant portion of the crystals reorient at less than half of this strain. We attribute the rapid crystallite rotation to the presence of nanoporosity, visible in the images, which allows large local deformation of certain crystals and their rapid rotation. This presence of residual nanoscale porosity and deformed crystals is evident in Figure 9, which is a thinned section of a pillar after axial compression to ≈40% reduction. In the bulk region of this pillar some of the crystallites exhibit (0002) planes aligned towards the principal shear direction (45 ° away from the loading axis), while the crystallites near the substrate align their (0002) strongly with the interface. The crystals adjacent to porosity have their (0002) planes aligned most ideally with the principal shear direction. A similar phenomenon is observed during wear testing, where the crystals in the lower density material adjacent to the substrate rotate faster than the crystals in the higher density portion of the film above this region. During high cycle wear, the crystallinity of MoS_2 has also been shown to evolve and have an influence on the tribofilm properties.[18]

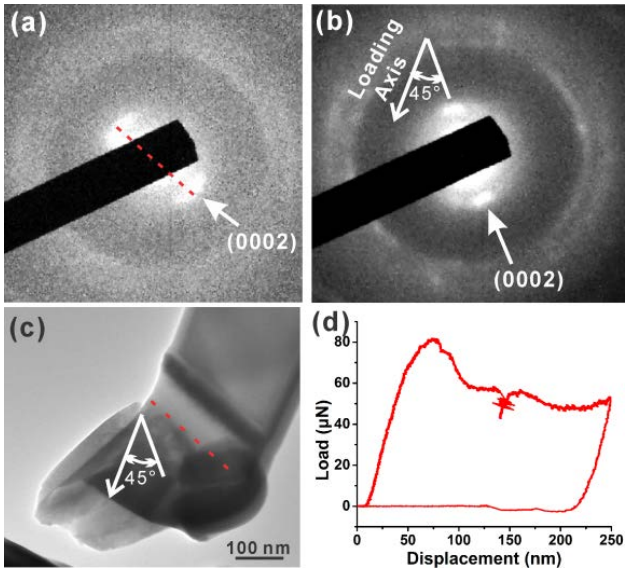

Figure 7. Structural change during compression of the pristine MoS_2 nanopillar. (a) Electron diffraction pattern of the MoS_2 pillar prior to compression (b) Electron diffraction pattern of the MoS_2 pillar after compression, showing increased crystalline ordering induced by the compression process (c) MoS_2 nanopillar after compression. (d) Load vs. displacement curve for the compression of this pristine MoS_2 nanopillar.

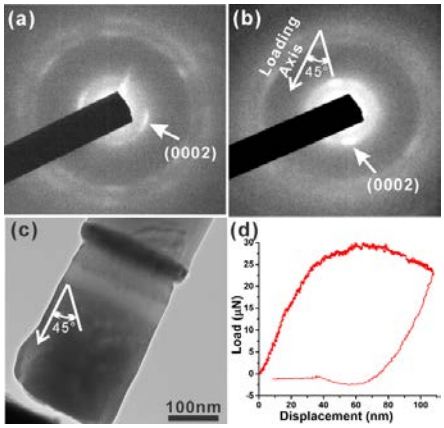

Figure 8. Structural change during compression of the 'pre-worn' MoS_2 nanopillar. (a) Electron diffraction pattern of the MoS_2 pillar prior to compression (b) Electron diffraction pattern of the MoS_2 pillar after compression, showing increased crystalline ordering induced by the compression process (c) MoS_2 nanopillar after compression. (d) Load vs. displacement curve for the compression of this 'pre-worn' MoS_2 nanopillar.

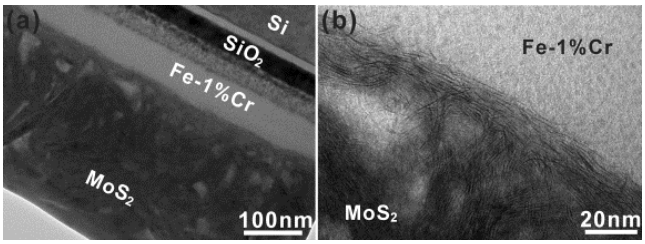

Figure 9. TEM cross-section of MoS_2 after compression by 40% at the interface between film and substrate showing (a) the Si/SiO_2/ Fe-1% Cr/ MoS_2 substrate layers and (b) the interface between MoS_2 and 1% Cr steel sublayer.

Discussion

The remarkable ability of the MoS_2 to self-optimize its structure and properties during wear underpins its efficacy as a solid lubricant. The three fundamental mechanical properties characterized - strength, modulus, and strain to failure, all improved markedly during pre-wear. Similarly, wear rate and coefficient of friction also improve as these properties evolve. The overall dynamic response derives from the ability of the MoS_2 crystallites to easily reorient to accommodate shear. The enhanced strength and modulus should derive from the densification occurring in the structure during wear, whose stress-state must have a sufficiently large hydrostatic component to avoid fracture, such as is observed during compression of the pristine material.

While it should be possible to improve strength and modulus of MoS_2 by producing denser films, our results suggest that the presence of residual porosity plays an important role in facilitating crystallite rotation. This rotation is important to allow the crystallites to align in a direction that best accommodates strain, which differs significantly from the pristine texture. In a prior study, we examined the effect of chromium doping on the mechanical properties of MoS_2 tested in the pristine state. While doping enhanced strength, it also significantly altered the porosity and crystallite size.[12] Dry-sliding wear performed on those samples indicates that the samples with high porosity, a refined crystallite size, and refined pore size provided the lowest coefficients of friction and wear rates. Those results are consistent with the current work demonstrating the importance of the residual porosity in facilitating self-optimization of the microstructure and properties during wear.

Recent work on wear in alloys indicates that metals that self-organize into layered structures that facilitate shear provide significantly enhanced wear properties relative to chemically identical systems that do not.[21] This is contrary to Archads' rule, even when the latter alloys have higher hardness. The situation qualitatively mirrors the current results, where producing a microstructure that can self-optimize during wear leads to superior properties. Our characterization reveals that residual porosity plays a key role in facilitating the natural tendency of MoS_2 to evolve towards a more idealized microstructure with enhanced wear resistance, reduced coefficient of friction, and superior mechanical properties.

Conclusions

A combination of controlled dry sliding wear tests and *in-situ* site specific nanomechanical testing reveals the natural tendency of the MoS_2 microstructure to respond to wear in a manner that accommodates strain and enhances mechanical properties. This self-optimization characteristic is hypothesized to be critical in the material's success as a solid-lubricant. We also note that residual porosity and crystallite size play an important role in governing the associated microstructural evolution, and could be manipulated to promote or supress the ability of the material to self-optimize.

AUTHOR INFORMATION

Corresponding Authors

Prof. Shen J. Dillon E-mail: sdillon@illinois.edu

Prof. Paul O'Brien

E-mail: Paul.O'Brien@manchester.ac.uk

ACKNOWLEDGMENT

The authors would like to acknowledge the funding and support of the BP International Centre for Advanced Materials (BP-ICAM) that facilitated the collaboration in this research. Some of the instrumentation used was funded by the U.K. Engineering and Physical Sciences Research Council (grant number EP/K039547/1). All research data supporting this publication are directly available within this publication. The authors declare no competing financial interests.

REFERENCES

1. Winer, W. O., Molybdenum Disulfide as a Lubricant. *Wear* **1967,** *10* (6), 422-452.
2. Rapoport, L.; Leshchinsky, V.; Lapsker, I.; Volovik, Y.; Nepomnyashchy, O.; Lvovsky, M.; Popovitz-Biro, R.; Feldman, Y.; Tenne, R., Tribological Properties of WS_2 Nanoparticles Under Mixed Lubrication. *Wear* **2003,** *255* (Pt. 2), 785-793.
3. Watanabe, S.; Noshiro, J.; Miyake, S., Tribological Characteristics of WS2/MoS2 solid lubricating multilayer films. *Surf. Coat. Technol.* **2004,** *183* (2-3), 347-351.
4. Kimura, Y.; Wakabayashi, T.; Okada, K.; Wada, T.; Nishikawa, H., Boron Nitride as a Lubricant Additive. *Wear* **1999,** *232* (2), 199-206.
5. Dienwiebel, M.; Pradeep, N.; Verhoeven, G. S.; Zandbergen, H. W.; Frenken, J. W. M., Model Experiments of Superlubricity of Graphite. *Surf. Sci.* **2005,** *576* (1-3), 197-211.
6. Miro, P.; Audiffred, M.; Heine, T., An Atlas of Two-Dimensional Materials. *Chem. Soc. Rev.* **2014,** *43* (18), 6537-6554.
7. De Barros Bouchet, M. I.; Martin, J. M.; Le Mogne, T.; Bilas, P.; Vacher, B.; Yamada, Y., Mechanisms of MoS_2 Formation by MoDTC in Presence of ZnDTP: Effect of Oxidative Degradation. *Wear* **2005,** *258* (11–12), 1643-1650.
8. Kosarieh, S.; Morina, A.; Lainé, E.; Flemming, J.; Neville, A., The Effect of MoDTC-type Friction Modifier on the Wear Performance of a Hydrogenated DLC Coating. *Wear* **2013,** *302* (1–2), 890-898.
9. Savan, A.; Pfluger, E.; Voumard, P.; Schroer, A.; Simmonds, M., Modern Solid Lubrication: Recent Developments and Applications of MoS_2. *Lubr. Sci.* **2000,** *12* (2), 185-203.
10. Voumard, P.; Savan, A.; Pfluger, E., Advances in Solid Lubrication with MoS_2 Multilayered Coatings. *Lubr. Sci.* **2001,** *13* (2), 135-145.
11. Ding, X.-Z.; Zeng, X. T.; He, X. Y.; Chen, Z., Tribological Properties of Cr- and Ti-Doped MoS_2 Composite Coatings Under Different Humidity Atmosphere. *Surf. Coat. Technol.* **2010,** *205* (1), 224-231.
12. Tedstone, A. A.; Lewis, D. J.; Hao, R.; Mao, S.-M.; Bellon, P.; Averback, R. S.; Warrens, C. P.; West, K. R.; Howard, P.; Gaemers, S.; Dillon, S. J.; O'Brien, P., Mechanical Properties of Molybdenum Disulfide and the Effect of Doping: An in Situ

TEM Study. *ACS Appl. Mater. Interfaces* **2015,** *7* (37), 20829-20834.
13. Fleischauer, P. D., Effects of Crystallite Orientation on Environmental Stability and Lubrication Properties of Sputtered MoS2 Thin Films. *ASLE Trans.* **1984,** *27* (1), 82-88.
14. Chromik, R. R.; Baker, C. C.; Voevodin, A. A.; Wahl, K. J., *In Situ* Tribometry of Solid Lubricant Nanocomposite Coatings. *Wear* **2007,** *262* (9-10), 1239-1252.
15. Lahouij, I.; Dassenoy, F.; Knoop, L.; Martin, J.-M.; Vacher, B., In Situ TEM Observation of the Behavior of an Individual Fullerene-Like MoS_2 Nanoparticle in a Dynamic Contact. *Tribol. Lett.* **2011,** *42* (2), 133-140.
16. Oviedo, J. P.; Kc, S.; Lu, N.; Wang, J.; Cho, K.; Wallace, R. M.; Kim, M. J., In Situ TEM Characterization of Shear-Stress-Induced Interlayer Sliding in the Cross Section View of Molybdenum Disulfide. *ACS Nano* **2015,** *9* (2), 1543-1551.
17. Moser, J.; Levy, F., Molybdenum sulfide (MoS_{2-x}) Lubricating Films: Structure and Wear Mechanisms Investigated by Cross-Sectional Transmission Electron Microscopy. *Thin Solid Films* **1993,** *228* (1-2), 257-260.
18. Lahouij, I.; Vacher, B.; Martin, J.-M.; Dassenoy, F., IF-MoS2 based lubricants: Influence of Size, Shape and Crystal Structure. *Wear* **2012,** *296* (1-2), 558-567.
19. Lahouij, I.; Vacher, B.; Dassenoy, F., Direct Observation by *in situ* Transmission Electron Microscopy of the Behaviour of IF-MoS2 Nanoparticles During Sliding Tests: Influence of the Crystal Structure. *Lubr. Sci.* **2014,** *26* (3), 163-173.
20. Lewis, D. J.; Tedstone, A. A.; Zhong, X. L.; Lewis, E. A.; Rooney, A.; Savjani, N.; Brent, J. R.; Haigh, S. J.; Burke, M. G.; Muryn, C. A.; Raftery, J. M.; Warrens, C.; West, K.; Gaemers, S.; O'Brien, P., Thin Films of Molybdenum Disulfide Doped with Chromium by Aerosol-Assisted Chemical Vapor Deposition (AACVD). *Chem. Mater.* **2015,** *27* (4), 1367-1374.
21. Ren, F.; Arshad, S. N.; Bellon, P.; Averback, R. S.; Pouryazdan, M.; Hahn, H., Sliding Wear-Induced Chemical Nanolayering in Cu–Ag, and its Implications for High Wear Resistance. *Acta Mater.* **2014,** *72*, 148-158.

TABLE OF CONTENTS GRAPHIC